

REGULARIZED SHALLOW WATER EQUATIONS APPLIED TO FLOWS WITH WET/DRY BOTTOM AREAS

Oleg V. Bulatov¹, Tatiana G. Elizarova² and Jean-Claude Lengrand³

¹Moscow State University, Faculty of Physics
e-mail: dombulatov@mail.ru

²Keldysh Institute of Applied Mathematics RAS
e-mail: telizar@yahoo.com

³CNRS/ICARE, 1C, av. de la recherche scientifique, 45071 Orléans cedex 2
e-mail: jc.lengrand@orange.fr

Keywords: hydraulics, shallow water, regularization, finite-volume method, wet/dry areas, tsunami

Abstract. *A new well-balanced finite-volume algorithm for solving shallow water equations is presented together with its extension to wet/dry bottom conditions. 1D and 2D test problems are calculated and their comparison with analytical solutions and experimental data concerning tsunami propagation are presented.*

1 Introduction

In [1] a new and efficient numerical method to solve shallow water equations was proposed and tested. This method is based on a specific form of averaging shallow water equations over a small period of time, that results in so-called regularized shallow water (RSW) equations. The RSW numerical simulation of a hydraulic jump is presented in [2]. The RSW system can be regarded as a barotropic approximation for the Quasi-Gas Dynamic (QGD) equations obtained before e.g. [3]. The QGD equations were used for numerical calculations of a wide range of hydrodynamic problems, where they demonstrated their efficiency. The numerical algorithm implements a finite volume form and is explicit in time, which is favorable for non-stationary flow modeling and is easily adapted for parallel computations. This method was naturally generalized for unstructured meshes.

In this paper the RSW algorithm is briefly presented and developed for "wet/dry bottom" boundary conditions. The RSW finite-volume algorithm is tested for the one-dimensional test problem of preservation of still water surface at a surface-piercing hump to demonstrate the well-balance property of the scheme. The non-stationary 1D problems of dam break with flat dry bottom and tsunami runup on a plane beach show a good quality of the numerical solution and its convergence to the etalon results when decreasing the computational space step.

We propose a way to set boundary conditions for a 2D non-stationary "wet/dry bottom" problems and show their implementations for 2D tsunami runup onto a complex beach.

2 Regularized shallow water (RSW) equations

Obtaining the RSW equations starts with the plane 2D shallow water (SW) equations in the flux form

$$\frac{\partial h}{\partial t} + \frac{\partial u_x h}{\partial x} + \frac{\partial u_y h}{\partial y} = 0, \quad (1)$$

$$\frac{\partial h u_x}{\partial t} + \frac{\partial}{\partial x} \left(h u_x^2 + \frac{1}{2} g h^2 \right) + \frac{\partial}{\partial y} (h u_x u_y) = h f_x - g h \frac{\partial b}{\partial x}, \quad (2)$$

$$\frac{\partial h u_y}{\partial t} + \frac{\partial}{\partial x} (h u_x u_y) + \frac{\partial}{\partial y} \left(h u_y^2 + \frac{1}{2} g h^2 \right) = h f_y - g h \frac{\partial b}{\partial y}. \quad (3)$$

The unknown functions in (1) – (3) are the water level $h(x, y, t)$ measured from the known bottom profile $b(x, y)$, and velocity components $u_x(x, y, t)$ and $u_y(x, y, t)$. Here $g = 9.81 \text{ m/s}^2$ is the gravity acceleration, f_x, f_y are the components of external volume forces.

To construct the regularized equations we average Eqs. (1) – (3) over a small time interval Δt . We introduce the "tilded" values for water level h and velocities u_i , that relate them to intermediate time level $t < \tilde{t} < t + \Delta t$, so $\tilde{h}(x, y, t) = h(x, y, \tilde{t})$, and $\tilde{u}_x(x, y, t) = u_x(x, y, \tilde{t})$, $\tilde{u}_y(x, y, t) = u_y(x, y, \tilde{t})$. This time change is supposed to be small, and if the corresponding derivatives are smooth enough, then the "tilded" values can be estimated using the first term of the Taylor series in time as

$$\tilde{h} = h + \tau \frac{\partial h}{\partial t}, \quad \tilde{u}_i = u_i + \tau \frac{\partial u_i}{\partial t}, \quad (4)$$

where $0 < \tau < \Delta t$. We suppose that τ is the same for all terms and drop the terms of order $O(\tau^2)$.

The resulting RSW equations are:

$$\frac{\partial h}{\partial t} + \frac{\partial j_{mx}}{\partial x} + \frac{\partial j_{my}}{\partial y} = 0, \quad (5)$$

$$\frac{\partial hu_x}{\partial t} + \frac{\partial j_{mx}u_x}{\partial x} + \frac{\partial j_{my}u_x}{\partial y} + \frac{\partial}{\partial x}\left(\frac{gh^2}{2}\right) = h^*(f_x - g\frac{\partial b}{\partial x}) + \frac{\partial \Pi_{xx}}{\partial x} + \frac{\partial \Pi_{yx}}{\partial y}, \quad (6)$$

$$\frac{\partial hu_y}{\partial t} + \frac{\partial j_{mx}u_y}{\partial x} + \frac{\partial j_{my}u_y}{\partial y} + \frac{\partial}{\partial y}\left(\frac{gh^2}{2}\right) = h^*(f_y - g\frac{\partial b}{\partial y}) + \frac{\partial \Pi_{xy}}{\partial x} + \frac{\partial \Pi_{yy}}{\partial y}, \quad (7)$$

where

$$h^* = h - \tau\left(\frac{\partial hu_x}{\partial x} + \frac{\partial hu_y}{\partial y}\right). \quad (8)$$

Here

$$j_{mx} = h(u_x - w_x), \quad j_{my} = h(u_y - w_y), \quad (9)$$

and

$$w_x = \frac{\tau}{h}\left(\frac{\partial(hu_x^2)}{\partial x} + \frac{\partial(hu_xu_y)}{\partial y} + gh\frac{\partial h}{\partial x} + gh\frac{\partial b}{\partial x} - hf_x\right), \quad (10)$$

$$w_y = \frac{\tau}{h}\left(\frac{\partial(hu_xu_y)}{\partial x} + \frac{\partial(hu_y^2)}{\partial y} + gh\frac{\partial h}{\partial y} + gh\frac{\partial b}{\partial y} - hf_y\right), \quad (11)$$

$$\begin{aligned} \Pi_{xx} = \tau hu_x \left(u_x \frac{\partial u_x}{\partial x} + u_y \frac{\partial u_x}{\partial y} + g \frac{\partial h}{\partial x} + g \frac{\partial b}{\partial x} - f_x \right) + \\ \tau gh \left(u_x \frac{\partial h}{\partial x} + u_y \frac{\partial h}{\partial y} + h \frac{\partial u_x}{\partial x} + h \frac{\partial u_y}{\partial y} \right), \end{aligned} \quad (12)$$

$$\Pi_{yx} = \tau u_y h \left(u_x \frac{\partial u_x}{\partial x} + u_y \frac{\partial u_x}{\partial y} + g \frac{\partial h}{\partial x} + g \frac{\partial b}{\partial x} - f_x \right) \quad (13)$$

$$\Pi_{xy} = \tau u_x h \left(u_x \frac{\partial u_y}{\partial x} + u_y \frac{\partial u_y}{\partial y} + g \frac{\partial h}{\partial y} + g \frac{\partial b}{\partial y} - f_y \right) \quad (14)$$

$$\begin{aligned} \Pi_{yy} = \tau hu_y \left(u_x \frac{\partial u_y}{\partial x} + u_y \frac{\partial u_y}{\partial y} + g \frac{\partial h}{\partial y} + g \frac{\partial b}{\partial y} - f_y \right) + \\ \tau gh \left(u_x \frac{\partial h}{\partial x} + u_y \frac{\partial h}{\partial y} + h \frac{\partial u_x}{\partial x} + h \frac{\partial u_y}{\partial y} \right). \end{aligned} \quad (15)$$

The RSW equations can be regarded as the extension of the classical SW system. The SW and RSW systems differ by terms of $O(\tau)$. For $\tau \rightarrow 0$ the RSW system reduces to the SW system and smooth solutions of RSW system are also expected to converge to the corresponding solutions of SW system. For stationary problems if functions $u_x(x, y)$, $u_y(x, y)$ and $h(x, y)$ are solutions of the stationary SW equations, they are also solutions of the stationary RSW equations.

3 Numerical algorithm for 1D flows

For a plane one-dimensional flow RSW equations write as

$$\frac{\partial h}{\partial t} + \frac{\partial j_m}{\partial x} = 0, \quad (16)$$

$$\frac{\partial hu}{\partial t} + \frac{\partial j_m u}{\partial x} + \frac{\partial}{\partial x} \left(\frac{gh^2}{2} \right) = \left(h - \tau \frac{\partial hu}{\partial x} \right) \cdot \left(f - g \frac{\partial b}{\partial x} \right) + \frac{\partial \Pi}{\partial x}, \quad (17)$$

where

$$j_m = h(u - w), \quad (18)$$

$$w = \frac{\tau}{h} \left(\frac{\partial hu^2}{\partial x} + gh \frac{\partial h}{\partial x} + gh \frac{\partial b}{\partial x} - hf \right), \quad (19)$$

$$\Pi = \tau uh \left(u \frac{\partial u}{\partial x} + g \frac{\partial h}{\partial x} + g \frac{\partial b}{\partial x} - f \right) + \tau gh \left(u \frac{\partial h}{\partial x} + h \frac{\partial u}{\partial x} \right). \quad (20)$$

Following the numerical method for QGD equations, e.g. [3], the numerical algorithm for RSW Eqs. (16) – (20) uses a finite-volume approach with central-difference approximation for all fluxes included in the system. Time integration is made in explicit form. Unknown variables $h(x, t)$ and $u(x, t)$ are determined in the nodes i of a computational grid.

The values in the half-integer space points are

$$h_{i+1/2} = 0.5(h_i + h_{i+1}), \quad (21)$$

$$u_{i+1/2} = 0.5(u_i + u_{i+1}),$$

$$b_{i+1/2} = 0.5(b_i + b_{i+1}).$$

Using half-integer values we calculate the fluxes (18) – (20) as

$$j_{m,i+1/2} = h_{i+1/2}(u_{i+1/2} - w_{i+1/2}), \quad (22)$$

where, for a space grid with step Δx

$$w_{i+1/2} = \frac{\tau_{i+1/2}}{h_{i+1/2}} \left(\frac{h_{i+1}u_{i+1}^2 - h_i u_i^2}{\Delta x} + gh_{i+1/2} \frac{h_{i+1} - h_i}{\Delta x} + gh_{i+1/2} \frac{b_{i+1} - b_i}{\Delta x} - h_{i+1/2} f_{i+1/2} \right)$$

In the same way

$$\begin{aligned} \Pi_{i+1/2} = \tau_{i+1/2} u_{i+1/2} h_{i+1/2} & \left(u_{i+1/2} \frac{u_{i+1} - u_i}{\Delta x} + g \frac{h_{i+1} - h_i}{\Delta x} + g \frac{b_{i+1} - b_i}{\Delta x} - f_{i+1/2} \right) \\ & + \tau_{i+1/2} gh_{i+1/2} \left(u_{i+1/2} \frac{h_{i+1} - h_i}{\Delta x} + h_{i+1/2} \frac{u_{i+1} - u_i}{\Delta x} \right). \end{aligned}$$

As the last step we calculate the governing equations in the form

$$\frac{h_i^{k+1} - h_i^k}{\Delta t} + \frac{j_{m,i+1/2} - j_{m,i-1/2}}{\Delta x} = 0, \quad (23)$$

where k is the index corresponding to time-evolution with time step Δt . All space derivatives are calculated at time step k .

The flow rate equation (17) is approximated in the following way:

$$\begin{aligned} \frac{h_i^{k+1}u_i^{k+1} - h_i^k u_i^k}{\Delta t} + \frac{j_{m,i+1/2}u_{i+1/2} - j_{m,i-1/2}u_{i-1/2}}{\Delta x} + \frac{g}{2} \frac{h_{i+1/2}^2 - h_{i-1/2}^2}{\Delta x} \\ = h_i^* \left(f_i - g \frac{b_{i+1/2} - b_{i-1/2}}{\Delta x} \right) + \frac{\Pi_{i+1/2} - \Pi_{i-1/2}}{\Delta x}. \end{aligned} \quad (24)$$

Here

$$h_i^* = \frac{h_{i-1/2} + h_{i+1/2}}{2} - \tau_i \frac{h_{i+1/2}u_{i+1/2} - h_{i-1/2}u_{i-1/2}}{\Delta x}. \quad (25)$$

The proposed approximation for h_i^* values fulfills hydrostatic balance for the RSW numerical algorithm, that writes in the form: if $f(x, t) = 0$, $u(x, t) = 0$, then $h(x, t) + b(x, t) = \text{const}$.

The stability of the algorithm is provided by the terms in τ , where τ is related to the step grid Δx

$$\tau = \alpha \frac{\Delta x}{c}, \quad c = \sqrt{gh}. \quad (26)$$

Here $0 < \alpha < 1$ is a numerical factor chosen to ensure accuracy and stability of computations. τ is related to the time needed for a small perturbation to cross the computational cell. To improve stability, in supercritical flows c may be replaced by $c + |u|$.

The stability condition for the RSW algorithm has the Courant form, where the time step can be estimated as

$$\Delta t = \beta(\Delta x/c)_{\min}. \quad (27)$$

with Courant number $0 < \beta < 1$ to be adjusted to ensure convergence for the problem under consideration.

4 Boundary conditions for wet/dry bottom areas

In modern numerical approaches for implementing wet/dry bottom conditions a cut-off value of the water height ϵ is introduced, e.g.[4].

In the RSW algorithm we apply the cut-off condition as follows: if $h < \epsilon$ then $u = 0$ and $\tau = 0$; otherwise standard computations continue. For limited value of $\partial b/\partial x$ we relate the cut-off value ϵ to the slope of the bottom and to a space grid step Δx as

$$\epsilon \geq \Delta x \left| \left(\frac{\partial b}{\partial x} \right) \right|_{\max}. \quad (28)$$

In the computational algorithm the cut-off condition is applied to both integer and half-integer nodes of space grid.

These boundary conditions provide a well-balanced numerical solution of the RSW equations for wet/dry bottom flows as will be shown below.

5 Preservation of still water surface at a surface-piercing hump

This test is used to verify the well-balance property of the numerical scheme with wet/dry bottom areas, and is described in, e.g., [5] and [6].

In the 1D computational domain $L = 1\text{m}$ the bed topography is defined by

$$b(x) = \max\{0, 0.25 - 5(x - 0.5)^2\} \quad (29)$$

So a surface-piercing hump is located in the center of the computational domain as shown in Fig.1. All space dimensions are in meters.

Free surface level is given by $\xi(x) = \max\{0.1, b(x)\}$. The initial conditions provide the water inside the domain at rest. Boundary conditions for the left and right points of the domain are

$$\left. \frac{\partial h}{\partial x} \right|_{x=0,L} = 0, \quad u|_{x=0,L} = 0 \quad (30)$$

Numerical simulations are run up to $t = 200$ s. In computations two uniform space grids $\Delta x = 0.002$ m and $\Delta x = 0.001$ m are used. For both cases we choose $\alpha = 0.5$, $\beta = 0.5$ and $\epsilon = 0.01$. With such parameters, condition (28) is met. At $t = 0$ the hydrostatic balance condition $h_i + b_i = 0.1$ is also met for all points that belong to the water domain.

For both space grids water level stays at rest within the accuracy of the computational solution $\sim 10^{-6}$. Thus computations show that the RSW numerical algorithm is a well-balanced scheme.

6 Dam break in a channel with flat dry bottom. Comparison of numerical and analytical solutions

We consider a channel of length $L = 50$ m. A dam is situated at the center of the channel at $x = 25$ m. The initial data are

$$h(x)_{left} = 1\text{m}, \quad h(x)_{right} = 0, \quad u_0(x) = 0.$$

Soft boundary conditions are prescribed for h and u . The dam breaks at initial time.

Computations are provided up to time $t_{fin} = 5$ s using scheme parameters $\alpha = 0.2$, Courant number $\beta = 0.1$ and $\epsilon = 10^{-4}$. Here the regularization parameter is taken as $\tau = \alpha \Delta x / (\sqrt{gh} + |u|)$.

Fig. 2 shows the convergence of the numerical results for u (left) and h (right, fragment) to the analytical solution with grid refinement and 2 values of cut-off parameter ϵ . Decreasing ϵ brings the numerical solution close to the analytical one but requires a smaller time step.

7 Runup onto a plane beach.

This test was studied in [7]. Analytical solution for plane beach was obtained in [8] and was called Carrier and Greenspan periodic wave solution. Analytical solution for parabolic bed profile can be found in [9]. This test problem is frequently used for checking the ability of the algorithm to deal with run-up and run-down phenomenon. In particular this test helps to decide what sort of boundary condition should be set for a "moving shoreline".

For the analytical solution it is convenient to use non-dimensional variables

$$\begin{aligned} \tilde{x} &= x/L, \quad \tilde{\xi} = \xi/L \cdot \tan \gamma \\ \tilde{u} &= u/\sqrt{gL \cdot \tan \gamma}, \quad \tilde{t} = t/\sqrt{L/g \cdot \tan \gamma} \end{aligned} \quad (31)$$

The solution is written in implicit form

$$\begin{aligned} \tilde{u} &= -A \frac{J_1(\tilde{\sigma})}{\tilde{\sigma}} \sin(\tilde{\lambda}), \quad \tilde{x} = \tilde{\xi} - \frac{\tilde{\sigma}^2}{16} \\ \tilde{\xi} &= \frac{A}{4} J_0(\tilde{\sigma}) \cos(\tilde{\lambda}) - \frac{\tilde{u}^2}{4}, \quad \tilde{t} = \frac{\tilde{\lambda}}{2} - \tilde{u}. \end{aligned} \quad (32)$$

Here J_0 and J_1 stand for the Bessel functions of zero and first order, respectively. The expression is valid for $0 \leq A \leq 1$. We take a dimensionless amplitude $A = 0.6$, a length scale $L = 20$ m and beach slope $\tan \gamma = 1/30$. In numerical computations we choose the same parameters as for the analytical solution in [7]. Computations are carried out in the space domain $[-100, 10]$. (dimensions in meters) The initial free surface elevation at $t = 0$ was obtained by setting $t = 0$ in the analytical solution. Left boundary conditions for $\xi = b + h$ and u are also obtained from the analytical solution at $x = -100$ m.

Numerical computations were carried out for three uniform space grids $\Delta x = 0.1, 0.05$ and 0.025 m. For all space grids we set $\alpha = 0.2$ and $\beta = 0.1$. In this test ϵ was adapted to Δx to satisfy condition (28). The beach slope is $\tan \gamma = 1/30$, and ϵ is set equal to $\epsilon = \Delta x \cdot \tan \gamma$. Thereby we get $\epsilon = 1/300, 1/600$ and $1/1200$ m.

In Fig.3, left, the movement of the shoreline is shown for three time periods $3T$. The expression for time period T is derived from the analytical solution.

$$T = \pi \sqrt{L/(g \cdot \tan \gamma)} \quad (33)$$

The analytical solution is marked by a solid line, numerical results are marked by dashed lines. hx stands for Δx .

Differences between the three numerical solutions are noticeable only near peaks, as seen in Fig.3, right. The numerical results converge to the analytical solution with the decrease of grid step.

The velocity profile at $t = 5$ s is shown in Fig.4. Here we also compare analytical solution and numerical results for $\Delta x = 0.1, 0.05$ and 0.025 m. In Fig.4, right, a fragment of the velocity profile is shown for space domain $[-3, 3]$ m. This domain is located near the shoreline, so we can see how the velocity jump is reproduced in the numerical solution.

We should note two remarks. Firstly, due to the cut-off condition we do not know the exact position of the shoreline. That is why numerical results are shifted to the left. Secondly, the leap of velocity in numerical computations is smoothed, and near the shoreline, the velocity profile tries to reach the dry bottom value $u = 0$.

By decreasing the spatial grid step we improve numerical results, as shown in Fig.4, right. Thus grid convergence is demonstrated. Introducing a cut-off value for height and an additional condition for ϵ we get numerical results that agree closely with the analytical solution.

8 Tsunami runup onto a plane beach

This problem was presented as a test case in "The third international workshop on long-wave runup models" (Benchmark Problem N1). Problem definition and analytical results are given in: http://isec.nacse.org/workshop/2004_cornell/bmark1/html, [10].

At $t = 0$ the fluid in the domain is at rest. Initial free surface evaluation level $\xi = b + h$ is shown in Fig. 5. Analytical results are presented for ξ and u at times $t_1 = 160$ s, $t_2 = 175$ s and $t_3 = 220$ s. Shoreline movement is presented for time domain $[0, 355]$ s.

Numerical computations are carried out for three space grids $\Delta x = 5$ m, 2 m and 1 m. We choose $\alpha = 0.4$ as an optimal parameter for this problem. For all simulations parameter $\beta = 0.5$ remains constant. In this test we also change ϵ in according to Δx (28) as it was done in the previous test. Here $\tan \gamma = 0.1$ defines beach slope.

In Fig.6 the time evolution of the moving shoreline is plotted in comparison with reference data. The group of figures 7 and 8 presents comparisons of reference and numerical results of free surface elevation at t_1, t_2 and t_3 . In each figure numerical results are shown for three space grids.

All figures show a good similarity of numerical and reference results. It is seen that improving space resolution makes the computational results closer to the reference free surface evaluation and shoreline.

9 2D computational algorithm

The numerical algorithm for 2D non-stationary flow problems with wet/dry bottom conditions is constructed based on the same approach as for the 1D algorithm above. It consists of a finite-volume method for system (5) – (8) with central-difference approximation of all spatial derivatives.

The finite-difference algorithm for (5) – (8) writes

$$\hat{h}_{i,j} = h_{i,j} - \frac{\Delta t}{\Delta x} (j_{i+1/2,j}^x - j_{i-1/2,j}^x) - \frac{\Delta t}{\Delta y} (j_{i,j+1/2}^y - j_{i,j-1/2}^y) \quad (34)$$

$$\begin{aligned} \hat{h}\hat{u}_x = hu_x + \frac{\Delta t}{\Delta x} (\Pi_{i+1/2,j}^{xx} - \Pi_{i-1/2,j}^{xx}) - \frac{\Delta t}{\Delta x} (u_{i+1/2,j}^x j_{i+1/2,j}^x - u_{i-1/2,j}^x j_{i-1/2,j}^x) - \\ - 0.5g \frac{\Delta t}{\Delta x} (h_{i+1/2,j}^2 - h_{i-1/2,j}^2) + \frac{\Delta t}{\Delta y} (\Pi_{i,j+1/2}^{yx} - \Pi_{i,j-1/2}^{yx}) - \\ - \frac{\Delta t}{\Delta y} (u_{i,j+1/2}^x j_{i,j+1/2}^y - u_{i,j-1/2}^x j_{i,j-1/2}^y) + \Delta t h_{i,j}^{*x} \cdot \left(f_{i,j}^x - g \frac{b_{i+1/2,j} - b_{i-1/2,j}}{\Delta x} \right) \end{aligned} \quad (35)$$

$$\begin{aligned} \hat{h}\hat{u}_y = hu_y + \frac{\Delta t}{\Delta x} (\Pi_{i+1/2,j}^{xy} - \Pi_{i-1/2,j}^{xy}) - \frac{\Delta t}{\Delta x} (u_{i+1/2,j}^y j_{i+1/2,j}^x - u_{i-1/2,j}^y j_{i-1/2,j}^x) + \\ + \frac{\Delta t}{\Delta y} (\Pi_{i,j+1/2}^{yy} - \Pi_{i,j-1/2}^{yy}) - \frac{\Delta t}{\Delta y} (u_{i,j+1/2}^y j_{i,j+1/2}^y - u_{i,j-1/2}^y j_{i,j-1/2}^y) - \\ - 0.5g \frac{\Delta t}{\Delta y} (h_{i,j+1/2}^2 - h_{i,j-1/2}^2) + \Delta t h_{i,j}^{*y} \cdot \left(f_{i,j}^y - g \frac{b_{i,j+1/2} - b_{i,j-1/2}}{\Delta y} \right). \end{aligned} \quad (36)$$

Here $h_{i,j}^{*x}$ and $h_{i,j}^{*y}$ are calculated as

$$\begin{aligned} h_{i,j}^{*x} = 0.5(h_{i+1/2,j} + h_{i-1/2,j}) - \tau_{i,j} \left(\frac{h_{i+1/2,j} u_{i+1/2,j}^x - h_{i-1/2,j} u_{i-1/2,j}^x}{\Delta x} + \right. \\ \left. + \frac{h_{i,j+1/2} u_{i,j+1/2}^y - h_{i,j-1/2} u_{i,j-1/2}^y}{\Delta y} \right) \end{aligned} \quad (37)$$

$$\begin{aligned} h_{i,j}^{*y} = 0.5(h_{i,j+1/2} + h_{i,j-1/2}) - \tau_{i,j} \left(\frac{h_{i+1/2,j} u_{i+1/2,j}^x - h_{i-1/2,j} u_{i-1/2,j}^x}{\Delta x} + \right. \\ \left. + \frac{h_{i,j+1/2} u_{i,j+1/2}^y - h_{i,j-1/2} u_{i,j-1/2}^y}{\Delta y} \right) \end{aligned} \quad (38)$$

The proposed approximation provides the fulfillment of hydrostatic balance for the RSW numerical algorithm, that writes in the form: if $f^x = f^y = 0$, $u_x = u_y = 0$, then $h(x, y) + b(x, y) = \text{const}$. The finite-difference approximation for x and y components of j , w and Π are constructed in a similar way.

In the two-dimensional case the cut-off parameter ϵ is written in the form

$$\epsilon \geq \Delta x \left| \left(\frac{\partial b}{\partial x} \right) \right|_{x_0, y_0} + \Delta y \left| \left(\frac{\partial b}{\partial y} \right) \right|_{x_0, y_0}. \quad (39)$$

where $b(x_0, y_0)$ are the points on the water level. We can suggest different finite-difference approximations of this expression, but in practical computations a convenient expression is

$$\begin{aligned} \Delta_{i,j} &= |b_{i+1,j} - b_{i-1,j}| + |b_{i,j+1} - b_{i,j-1}| \\ \epsilon_{i,j} &= 3 \max\{\Delta_{i,j}, \Delta_{i\pm 1,j}, \Delta_{i,j\pm 1}, \Delta_{i\pm 1,j\pm 1}, \Delta_{i\pm 1,j\mp 1}\} \end{aligned} \quad (40)$$

10 Tsunami runup onto a complex three-dimensional beach

This test was also proposed in "The third international workshop on long-wave runup models" (Benchmark Problem N2). Here we simulated the laboratory experiment. Problem definition and experimental results were taken from: http://isec.nacse.org/workshop/2004_cornell/bmark1/html, - [10].

In this test the space domain has a length of 5.448m and a width of 3.402m. All sides of the domain except the left border are solid walls. An input wave (Fig.9, right) comes through the left side. The bed profile $b(x, y)$ is shown in Fig.9, left.

Barometry data, known from the experiment, are given in a space grid with cell size equal to 0.014 m and this value is taken as the computational space step $\Delta x = \Delta y$. Numerical parameters in the RSW algorithm are $\alpha = 0.1$ and $\beta = 0.1$. Simulation is run up to $t = 22$ s.

Fig.10, left shows the initial distribution for water level $h(x, y)$. Here white areas indicate the dry bottom (where $h(x, y) = 0$). Distribution for $h(x, y)$ at $t = 20$ s is shown in Fig.10.

In Fig.11 examples for h distributions together with streamlines are plotted for times 17 and 18 s. Here complicated unstationary flow patterns with a number of vortices are visible.

Figs. 12, 13 present the time-evolution of the free surface elevation in 3 reference points (Gauge 5: $(x, y) = (4.521, 1.196)$; Gauge 7: $(x, y) = (4.521, 1.696)$; Gauge 9: $(x, y) = (4.521, 2.196)$) measured in the experiment and compared with numerical results. Agreement of numerical and experimental time-distributions is clearly seen.

11 Conclusion

In this paper a new numerical method to solve shallow water equations is briefly described. The proposed method is based on the regularization of shallow water (RSW) system. Here the RSW method is completed by wet/dry bottom boundary conditions. The latter are written in a way that allows us to extend them to two-dimensional problems.

The RSW numerical method is tested for the one-dimensional test problem of preservation of still water surface at a surface-piercing bump to demonstrate the well-balance property of the scheme. The numerical simulations of dam break and two nonstationary problems of tsunami runup on a plane beach show a good quality of the numerical solution and its convergence to the etalon results when decreasing the computational space step and the cut-off parameter.

The RSW method and associated boundary conditions have been implemented for the two-dimensional space problem of tsunami runup onto a complex beach. It is calculated according to data obtained in the laboratory experiment. Excellent concordance with laboratory data are seen even for the time-evolution of the water level.

The obtained numerical results show the adequacy and perspectives of the proposed numerical RSW scheme.

This work has been supported by the Fund for Fundamental Researches of the Russian Academy of Science under reference 10-01-00136.

REFERENCES

- [1] T.G. Elizarova, O.V. Bulatov: Regularized shallow water equations and a new method of numerical simulation of the open channel flows. *Computers and Fluids*, N 46 (2011), 206–211.
- [2] Elizarova T.G., Lengrand J.C. A regularization method for the numerical solution of the shallow water equations. 5-th European Conference on Computational Fluid Dynamics ECCOMAS CFD 2010, Lisbon, Portugal, 14-17 June, 2010. Book of Abstracts, Eds. J.C.F.Pereira et al, vol.1, p.322. CD.
- [3] T.G. Elizarova: Quasi-Gas Dynamic Equations. Springer-Verlag, Berlin, 286 p, 2009.
- [4] M. Ricchiuto, A. Bollermann: Stabilized residual distribution for shallow water simulations. *J. Comput. Physics*, V. 228, N 4 (2009), 1071–1115.
- [5] Q. Liang, F. Marche: Numerical resolution of well-balanced shallow water equations with complex source terms. *Adv. Water Resources*, 32 (2009), 873-884.
- [6] T. Gallouet, J.M. Herard, N. Seguin: Some approximate Godunov schemes to compute shallow-water equations with topography. *Comp. Fluids*, 32 (2003), 479-513.
- [7] F. Marche: Theoretical and numerical study of shallow water models. Applications to nearshore hydrodynamics. PhD thesis, Universite de Bordeaux I, 2005.
- [8] G.F Carrier, H.P. Greenspan: Water waves of finite amplitude on a sloping beach. *J. Fluid Mech*, 4 (1958), 97–109.
- [9] W.C. Thacker: Some exact solutions to the nonlinear shallow-water wave equations. *J. Fluid Mech*, 107 (1981), 499–508.
- [10] [http : //isec.nacse.org/workshop/2004_cornell/bmark1/html](http://isec.nacse.org/workshop/2004_cornell/bmark1/html)

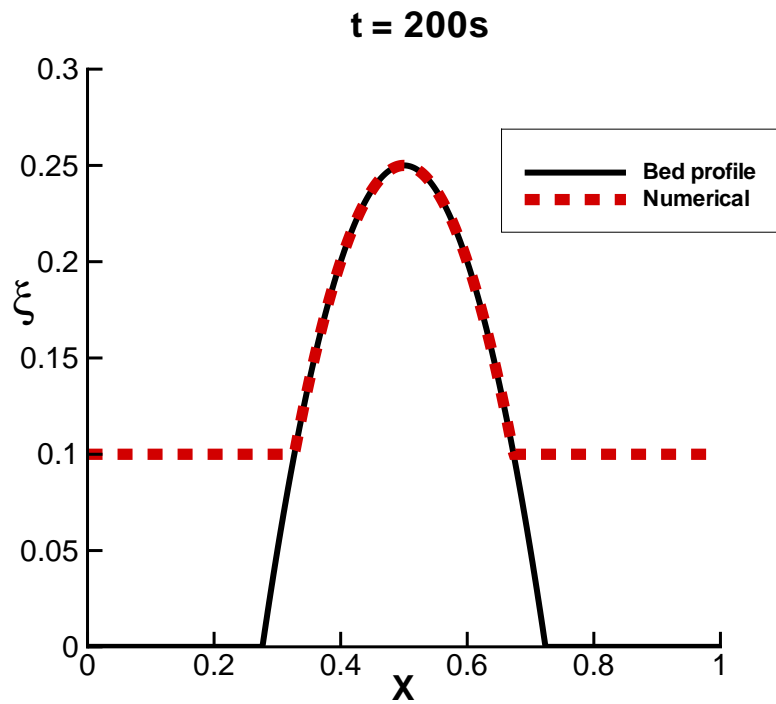


Figure 1: Undisturbed still water surface after $t = 200$ s

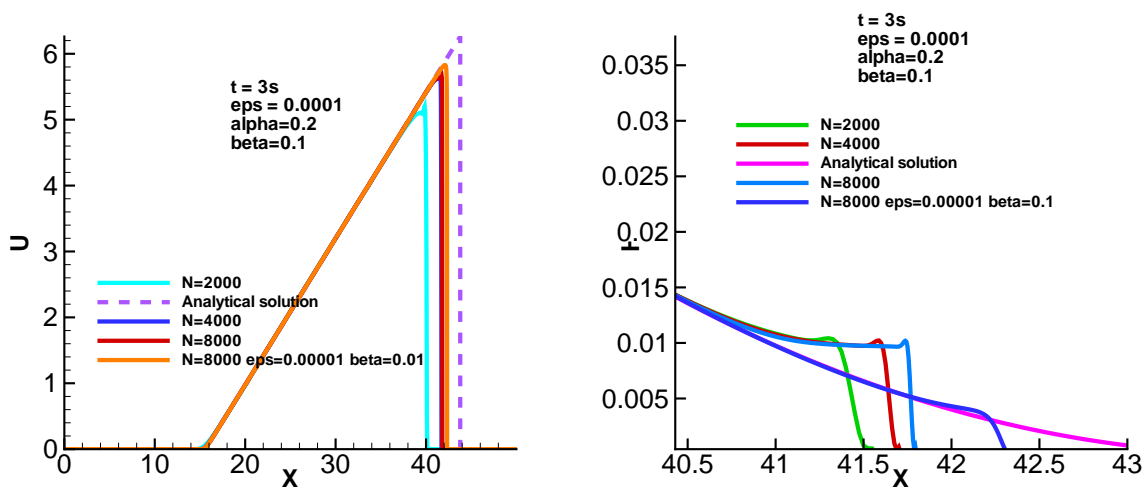


Figure 2: Dam break in dry bottom channel. Grid and cut-off parameter convergence

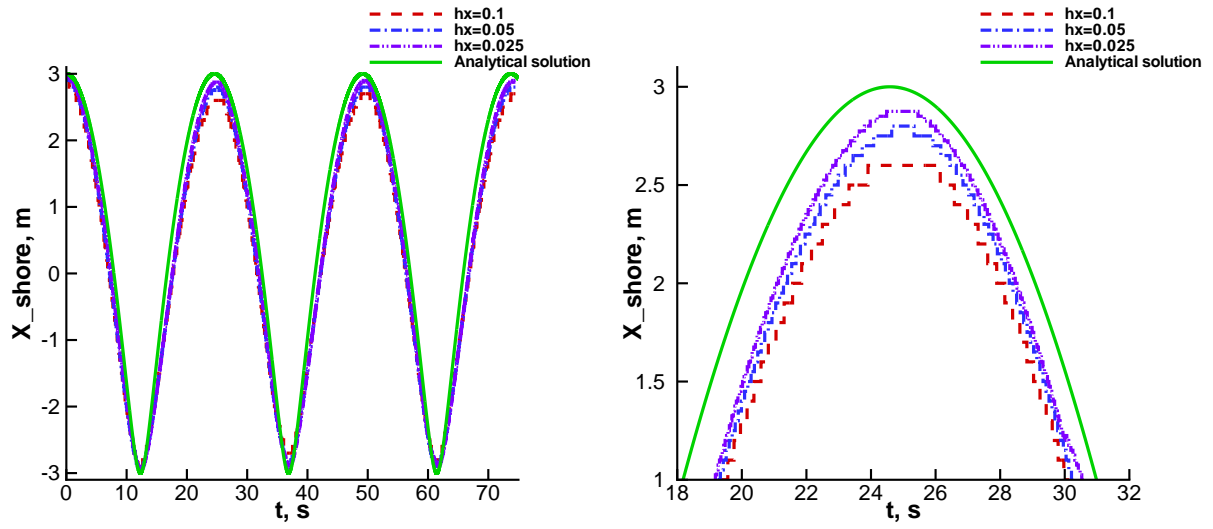


Figure 3: Shoreline movement for different space grids $\Delta x = 0.1$ m, $\Delta x = 0.05$ m, $\Delta x = 0.025$ m

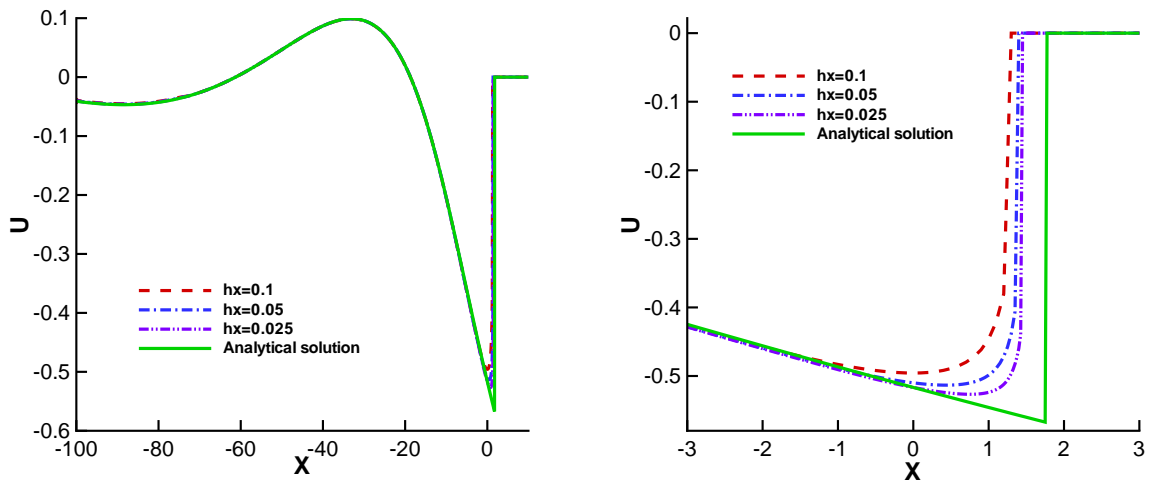


Figure 4: Left: velocity profile at $t = 5$ s for space grids $\Delta x = 0.1$ m, $\Delta x = 0.05$ m and $\Delta x = 0.025$ m. Right: fragment in the space domain $[-100, 10]$ with same space grids

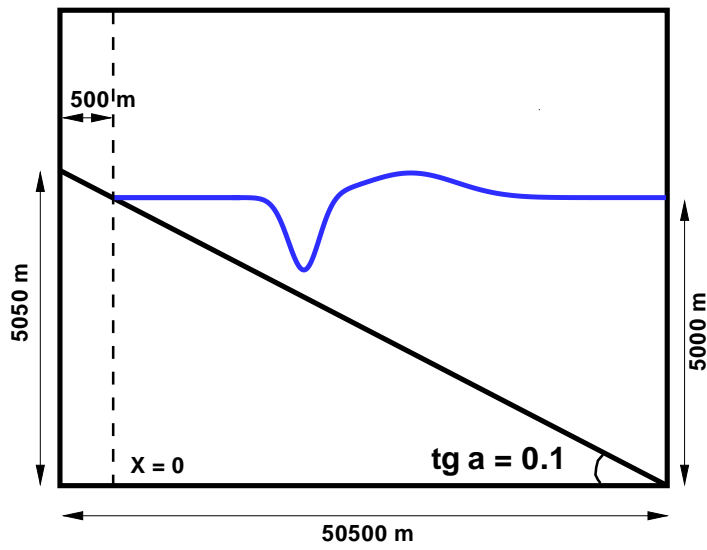


Figure 5: Initial level of free surface and domain set-up

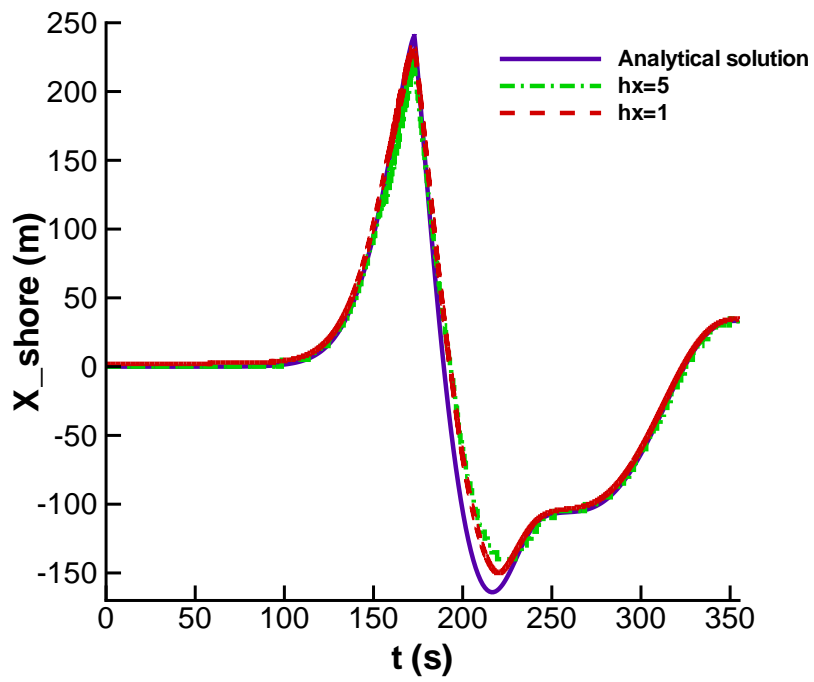


Figure 6: Shoreline movements for tsunami runup with space grids $\Delta x = 1$ m and, $\Delta x = 5$ m

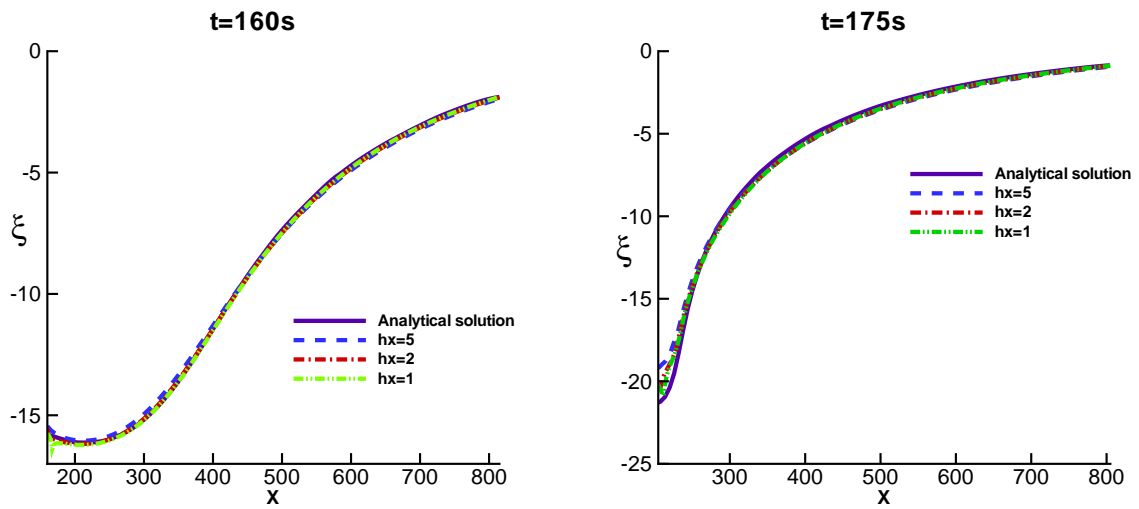


Figure 7: Analytical and numerical results of free surface level evaluation at $t = 160$ s (left) and $t = 175$ s (right) for space grids $\Delta x = 5$ m, $\Delta x = 2$ m and $\Delta x = 1$ m

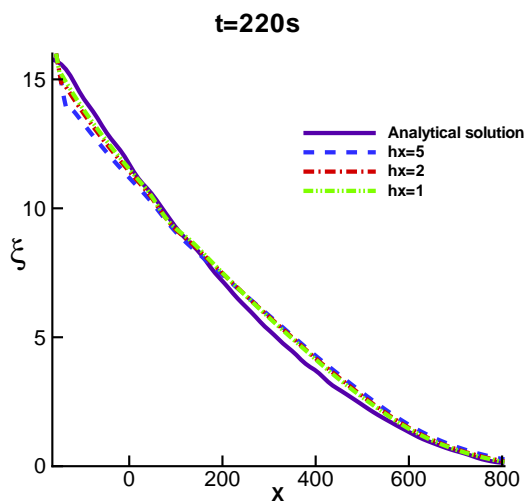


Figure 8: Analytical and numerical results for free surface level at $t = 220$ s for space grids $\Delta x = 5$ m, $\Delta x = 2$ m and $\Delta x = 1$ m

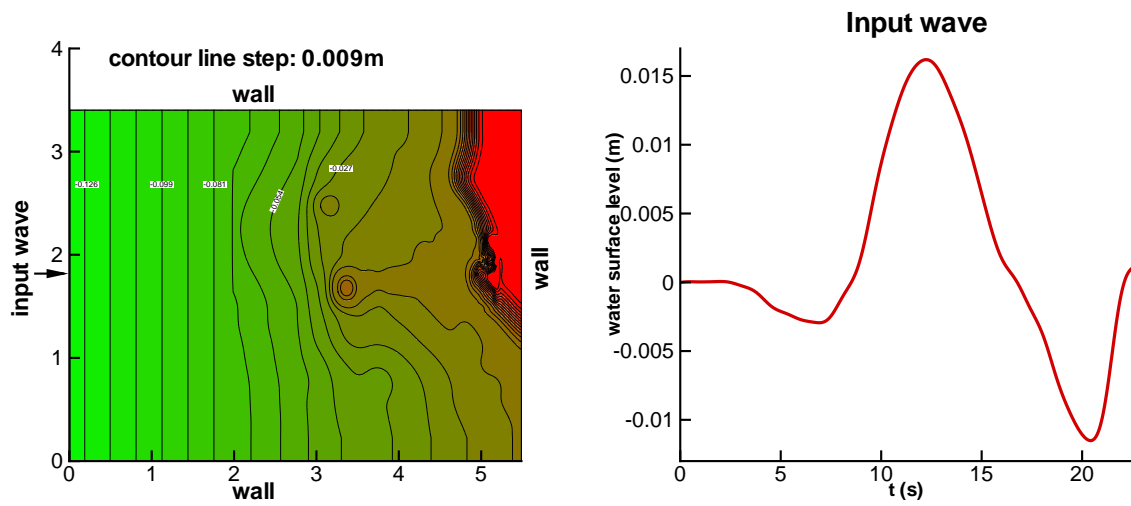


Figure 9: Bed profile (left) and incoming wave (right)

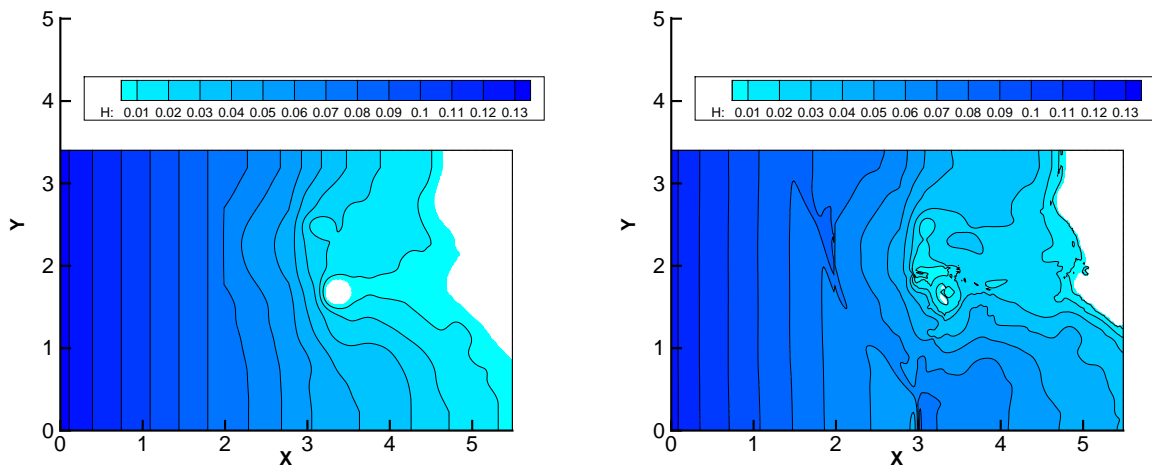


Figure 10: Distribution of water height h at $t = 0$ s (left) and $t = 20$ s (right)

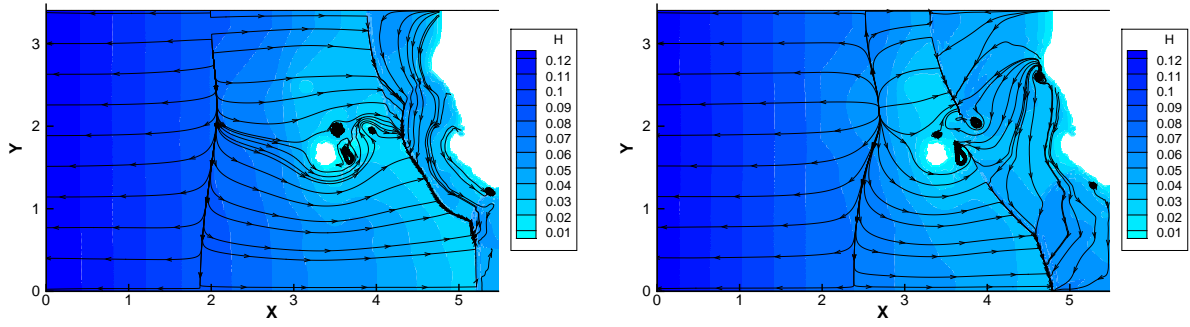


Figure 11: Distribution of h with streamlines at $t = 17$ s (left) and $t = 18$ s (right)

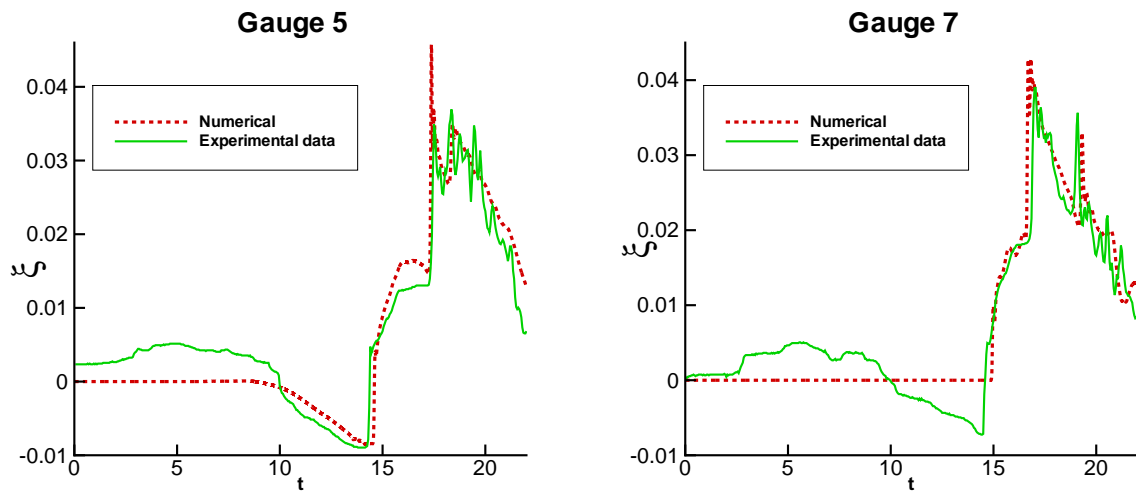


Figure 12: Time histories of free surface elevation at gauge 5 (left); $(x,y)=(4.521),(1.196)$ and gauge 7 (right); $(x,y)=(4.521),(1.696)$

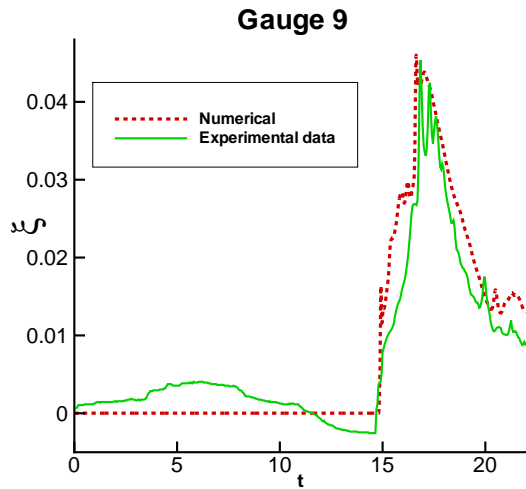


Figure 13: Time histories of free surface elevation at gauge 9; $(x,y)=(4.521),(2.196)$